Journal of Photochemistry and Photobiology A: Chemistry 220 (2011) 39–46

Contents lists available at ScienceDirect

Journal of Photochemistry and Photobiology A: Chemistry

journal homepage: www.elsevier.com/locate/jphotochem

Accessibility and shielding of silanol surface centers on porous silica beads; UV/vis absorption and fluorescence studies

Abeer S. Elsherbiny[a,*], Hans-J. Egelhaaf[b], Dieter Oelkrug[c]

[a] Chemistry Department, Science and Art College, King Abdulaziz University, Rabigh Campus, Rabigh 21911, Saudi Arabia
[b] Johannes-Kepler Univ./konarka Aust R&D, Christian-Doppler Lab Surface Optical Altenberger Str. 69, Linz, AT 4040, Austria
[c] Institute of Physical and Theoretical Chemistry, Tübingen University, Auf der Morgenstelle 8, 72076 Tübingen, Germany

ARTICLE INFO

Article history:
Received 12 December 2010
Received in revised form 22 February 2011
Accepted 12 March 2011
Available online 21 March 2011

Keywords:
Silica surface
Polymer coating
Adsorption equilibrium
Aza-aromatic adsorptives
Fluorescence anisotropy

ABSTRACT

The adsorption equilibria of proton accepting and donating analytes on porous silica beads applicable as stationary chromatographic phases were investigated by UV/vis absorption spectroscopy. Fluorescence spectroscopy was utilized to characterize the nature of the species formed at the silica surfaces after adsorption. In order to control the equilibria and states of adsorption the active silanol surface centers were partly shielded by adsorbed water or by two types of polymeric coatings, (i) polymerized 1,4-divinylbenzene (DVB) with loadings of 200 mg and 500 mg DVB/g silica, respectively, (ii) polymerized N,N′-diallyl-L-tartardiamide bis-(4-tertbutylbenzoate) (TBB) with a loading of 135 mg TBB/g silica. Acridine orange, 1,2,7,8-dibenzacridine, 3,4,5,6,-dibenzacridine, and lumichrome were used as fluorescent analytes with proton accepting or donating nitrogen centers. The fluorescence anisotropies show that the adsorbed species at the uncoated silica surface are highly immobilized. Coating considerably reduces the equilibrium constants of adsorption. polymerized N,N′-diallyl-L-tartardiamide bis-(4-tertbutylbenzoate) works much better than polymerized 1,4-divinylbenzene. In the latter case a large amount of polymer is necessary in order to produce a significant effect.

1. Introduction

Silica beads with diameters ranging from 10 nm to 100 μm are widely used e.g. as filling materials, adsorbents, catalytic supports, or stationary chromatographic phases. Nonporous, densely packed beads are obtained by flame hydrolysis (Aerosils), highly porous beads by liquid phase condensation. The condensation process leaves back some bulk water and silanol groups that cover almost the whole external and internal surfaces of the beads. In chromatography, silica-based materials have some disadvantages for the analysis of basic compounds because of the strong acid/base interaction between these compounds and the silanol groups of the support [1,2]. This type of interaction leads to tailing of the peaks in the chromatograms [3]. In order to overcome this unwanted effect, the mobile phases were optimized by careful adjustment of pH or addition of ionic substances [4,5]. However, ionic additives provide coverage of only one third of all the silanol groups [6–8]. Improved separation selectivity can also be obtained by tailoring the properties of the column packing materials [9,10]. End-capping is a process, whereby short-chain chlorosilanes are used to cover the silanol groups. However, even this process leaves some of the silanol groups unreacted. It is also possible to coat silica particles by means of a physically adsorbed polymer [11–13]. Hence, a reduction of unwanted analyte–silanol interactions is expected [14,15]. Polymer resins with a low degree of cross-linking suffer from mass transfer limitations as well as swelling problems, which can lead to poor chromatographic performance [16]. On the other hand, highly cross-linked styrene–divinylbenzene copolymers are generally less permeable for organic solvents and will therefore not swell to the same extent [17,18]. Therefore a thermal-initiated radical polymerization of pure styrene–divinylbenzene using dibenzoylperoxide as an initiator was used to coat porous and nonporous spherical silica particles [19,20]. N,N′-diallyl-L-tartardiamide bis-(4-tertbutylbenzoate) covalently bonded to Kromasil silica and crosslinked, has been used to separate enantiomers in analytical scale as well as in preparative scale [21,22].

In this paper the shielding of the surface silanol groups of chromatographic material by adsorbed water and organic polymer coatings is investigated with the methods of UV/vis-absorption and fluorescence spectroscopy. It has been shown that especially fluorescence spectroscopy is a very sensitive and selective tool to characterize chemical processes at the interfaces of stationary phases, such as molecular aggregation [23–25], electron transfer [26], proton transfer [27–31], or photochemical transfor-

* Corresponding author. Permanent address: Chemistry Department, Faculty of Science, Tanta University, 31527 Tanta, Egypt. Tel.: +20 40 3416038; fax: +20 40 3350804.
E-mail address: abeer.elsherbiny@yahoo.de (A.S. Elsherbiny).

1010-6030/$ – see front matter © 2011 Elsevier B.V. All rights reserved.
doi:10.1016/j.jphotochem.2011.03.011

mations [32]. Usually the micro-granular stationary phases are densely packed and thus subjected to multiple scattering and depolarization of the electromagnetic signals. We preserve polarization by investigating dilute bead suspensions, in the extreme case one bead only. The analytes were selected from a series of poly-conjugated heterocyclic fluorophores with potential proton accepting or donating nitrogen centers. The adsorption equilibria of these adsorptives were determined as function of the access to the surface silanol groups that act as weak proton donors, and of the acidity constants of the adsorptives that cover a wide range, $pK_a \approx 5$–11. The adsorbed states were characterized in detail by spectrally resolved fluorescence emission, excitation, polarization, and decay.

2. Theory (modeling of adsorption equilibria)

The adsorption reaction of the dissolved base B with the active centers S at the silica surface, and the desorption of the adsorbate complex BS is modeled in the simplest possible way

$$B + S \underset{k_{des}}{\overset{k_{ads}}{\rightleftarrows}} BS \tag{1}$$

where k_{ads} and k_{des} are the rate constants of adsorption and desorption, respectively. The equilibrium constant of reaction (1) is

$$K = \frac{k_{ads}}{k_{des}} = \frac{[BS]_{eq}}{[S]_{eq}[B]_{eq}} \tag{2}$$

where $[X]_{eq}$ are the equilibrium concentrations. Since we work with a large excess of S, its equilibrium concentration is not much different from its initial concentration, $[S]_{eq} \approx [S]_0$, and we rewrite Eq. (2)

$$K_{eff} = \frac{k_{eff}}{k_{des}} \approx \frac{[BS]_{eq}}{[B]_{eq}} \tag{3}$$

where $k_{eff} = k_{ads}\,[S]_0$ is the pseudo first order rate constant of adsorption. The adsorbate concentration *per area* can be substituted in highly porous adsorbents by concentration *per volume*, provided that the internal surface is accessible to B. In this case BS of Eq. (3) can be expressed by the difference of B before and after adsorption and by the ratio of the volume V_L of the liquid phase to the volume V_S of the solid phase

$$K_{eff} = \frac{k_{eff}}{k_{des}} \approx \left(\frac{[B]_0 - [B]_{eq}}{[B]_{eq}}\right)\frac{V_L}{V_S} \tag{4}$$

This equilibrium 'constant' is directly accessible from experimental data.

3. Experimental

3.1. Materials

Porous silica beads with specific surface area of 116 m^2/g, average particle diameter of 6 μm, and average pore size of 300 Å were obtained from Eka-Chemicals (Bohus-Sweden). The beads were (i) used without further pretreatment, (ii) preheated for 10 h in vacuum at $T = 150\,^{\circ}C$ prior to the room temperature adsorption experiments, (iii) coated with polymerized 1,4-divinylbenzene (DVB, see Fig. 1) at loadings of 200 mg and 500 mg DVB/g SiO_2; details of the sample preparation are exactly the same as for nonporous silica [33], (iv) coated with polymerized N,N′-diallyl-L-tartardiamide bis-(4-tertbutylbenzoate) (TBB, see Fig. 1) with a loading of 135 mg TBB/g SiO_2 as delivered from Eka-Chemicals.

The fluorescent adsorptives are depicted in Fig. 2. Acridine orange (AO) and lumichrome (LC) were from Aldrich, the two stereo-isomers 1,2,7,8-dibenzacridine (1-DBA) and 3,4,5,6-dibenzacridine (3-DBA) were a former gift from Perkampus et al. [34].

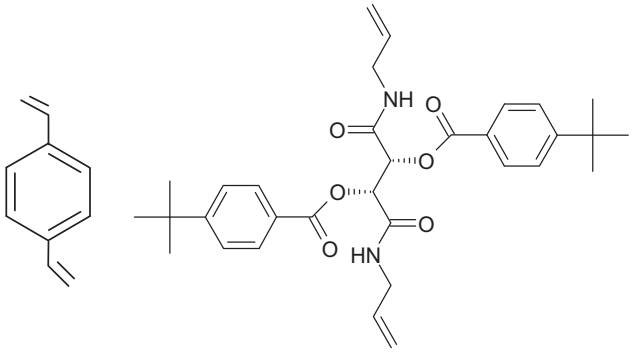

Fig. 1. Chemical structures of 1,4-divinylbenzene and N,N′-diallyl-L-tartardiamide bis-(4-tertbutylbenzoate) for polymeric coating of the silica beads.

The solvents for adsorption, dichloromethane (DCM) and cyclohexane (CH), both spectroscopic grades (Merck, Germany), were dried over zeolite and kept under dry nitrogen.

3.2. Procedures

Adsorption experiments were performed with 6 mg of silica beads suspended in 2 ml of DCM or CH in a 1 cm – fluorescence cell and stirred for 2 min under dry air. Then 1 ml of the adsorptive B in a solution of DCM or CH with the initial concentration $[B]_0 = 9 \times 10^{-7}$ to 7×10^{-6} mol L^{-1} was injected and stirred well. The equilibrium concentration $[B]_{eq}$ of the nonadsorbed adsorptive in solution was determined photometrically after centrifugation. In some cases the measurement was possible without centrifugation after sedimentation. Then the equilibrium constant K_{eff} of adsorption was calculated from Eq. (4).

Steady state fluorescence emission (F), fluorescence excitation (Exc), and fluorescence anisotropy (r_F) spectra were measured in the fluorometer SPEX Fluorolog 222, equipped with two double monochromators and Glan-Thompson polarizers (Instruments S.A., Longjumeau, France). The fluorescence cell containing the adsorbate suspension was stirred during the measurements in order to avoid sedimentation. The fluorescence anisotropy was evaluated in the conventional way from

$$r = \frac{I_{\parallel} - I_{\perp}}{I_{\parallel} + 2I_{\perp}} \tag{5}$$

where $I_{||}$ and $I_{\perp}$ are the fluorescence intensities parallel and perpendicular with respect to the polarization direction of the incident radiation.

Fluorescence decay curves were recorded in stirred suspensions with a time-correlated single-photon counting setup (pico-timing discriminators Ortec, model 9307, Time-to-Amplitude Converter Ortec, model 457, pre-amplifier (Ortec, model 9306) utilizing the emission monochromator of the fluorometer SPEX Fluorolog 222 and the photomultiplier tube (Ortec, model 9306). For excitation a picosecond diode laser (PicoQuant, Germany, model LDH-400 (371 nm), FWHM 70 ps) was used. Fluorescence lifetimes were obtained from a single to triple exponential analysis of the fluorescence intensity decay curves

$$I_F(t) = \sum\nolimits_i A_i \exp\left(\frac{-t}{\tau_{Fi}}\right) \tag{6}$$

where τ_{Fi} is the fluorescence decay time of the ith component, and A_i is the associated intensity amplitude at $t = 0$.

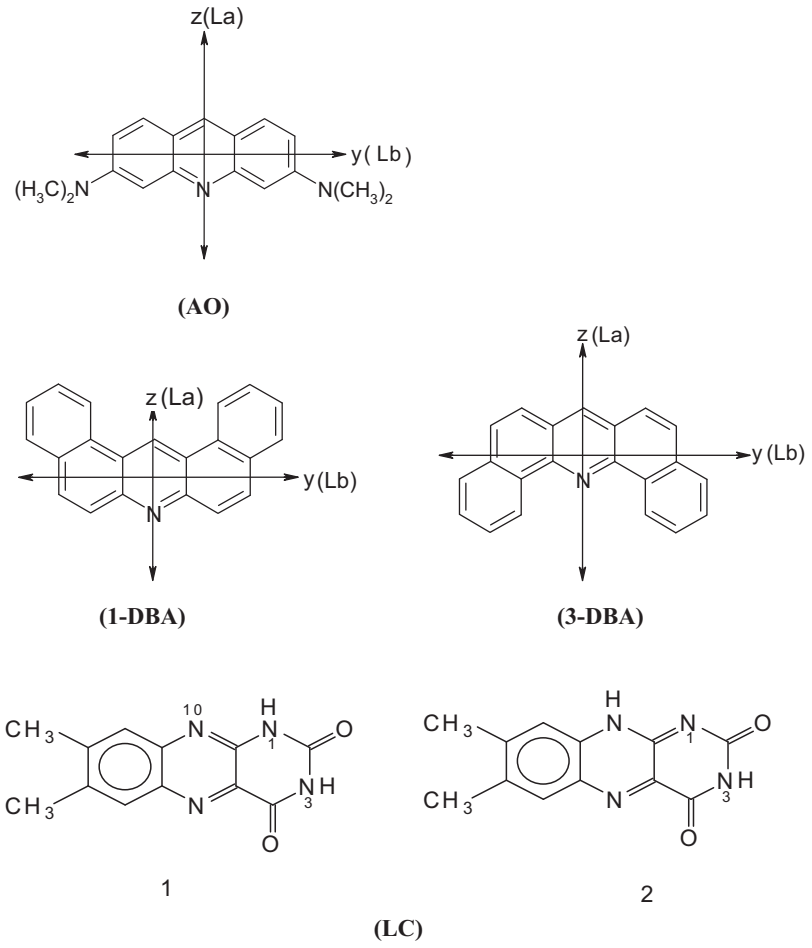

Fig. 2. Chemical structures of the adsorptives.

Analytical liquid chromatography is performed with a Merck-Hitachi 6200A solvent delivery pump and a Merck-Hitachi L-4000A variable wavelength UV detector. Samples are introduced via a Rheodyne injector equipped with a 20 μL loop. The mobile phases is used during the separations are mixtures of isopropanol/CH, and all analytes are dissolved in CH.

4. Results and discussion

4.1. Adsorption equilibria

All adsorption experiments were carried out with a large excess of liquid phase against solid phase ($V_L = 500V_S$) and adsorbate concentrations <3% of saturation capacity so that the equilibrium constants could be reliably evaluated with Eq. (4). Table 1 summarizes the most important results. On uncoated silica the equilibria depend strongly on the nature of the adsorptive. AO with its three basic nitrogen centers is very efficiently adsorbed whereas 3-DBA with its sterically shielded nitrogen atom remains almost completely in solution. The adsorptives LC and 1-DBA range between AO and 3-DBA. Extended experiments with 1-DBA show that traces of water play an important role for the value of K_{eff}. Adsorption from thoroughly dried CH yields a distinctly higher constant than adsorption from CH as supplied. Silica acts in the latter case as drying agent of the solvent. Since, at 20 °C and 50% r.h. the silica beads are covered with 20 mg H_2O/gram silica. This corresponds to a coverage of approximately 1×10^{-6} mol water/m^2, and this is roughly monolayer coverage. Thus all silanol groups are shielded by water and interaction with the nitrogen bases is possible only via Si–OH···H–O–H···N≡. The opposite effect is produced after pretreatment at 150 °C in vacuo. Under these conditions all physisorbed water disappears, but not the silanol OH-groups. So the preferential interaction is Si–OH···N═, with a higher probability of proton transfer, at least in the photoexcited singlet state.

The NIR absorption spectrum of Fig. 3 shows in this case the overtone of the unshielded ≡SiO–H valence vibration. After exposure to ambient atmosphere this band disappears and is replaced

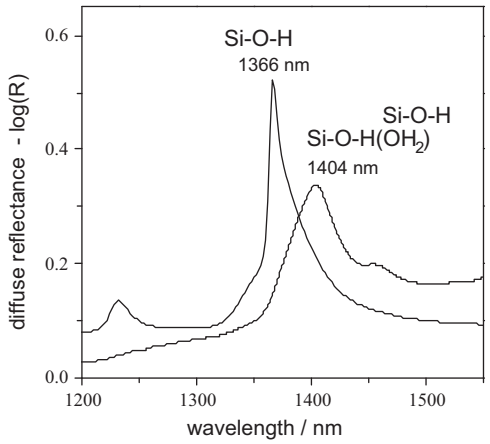

Fig. 3. NIR diffuse reflectance absorption spectra of porous silica powders in the region of the first SiO–H valence overtone. (1) Spectrum in a sealed cell after pretreatment at $T = 150$ °C in vacuum and (2) spectrum of the untreated powder.

Table 1
pK_a-values of the adsorptives in their S_0- and S_1-states [35–38]. Effective equilibrium constants of adsorption K_{eff} (see Eq. (4)) on uncoated and coated silica beads. The constants were measured for loadings 1×10^{-6} to 3.5×10^{-6} mol/g SiO_2.

Adsorptive adsorbed from	pK_a		K_{eff} on adsorbent			
	S_0	S_1	Uncoated silica	Coated silica		
			Pre-treatment	DVB		TBB-coating
				200/g	500 mg/g	135 mg/g
AO dry DCM	10.5	11.0	24,000 ± 3500	1500 ± 100	1100 ± 100	20 ± 5
	($BH^+ \leftrightarrow B + H^+$)					
1-DBA dry CH	5.5	10.7	Water removed at T_a = 150 °C			
	($BH^+ \leftrightarrow B + H^+$)		11,000 ± 2000 untreated 5700 ± 1000	–	–	<5
CH as supplied			Untreated 2000 ± 100	–	–	< 5
3-DBA dry CH	≈5		<10			< 1
LC dry DCM	≈8.6	3.6(N1)				
		7.5(N3)	2900 ± 250	320 ± 20	50 ± 10	60 ± 10
	($AH \leftrightarrow A^- + H^+$)					

at slightly longer wavelengths by the band of the shielded complex ≡SiO–H···OH_2. As a consequence the equilibrium constant of adsorbed 1-DBA decreases on humid silica by a factor of two against the thermally pretreated adsorbent (see Table 1).

High K_{eff}-values are certainly of advantage in the field of heterogeneous chemical transformations but not in the field of liquid chromatography. For practical applications one chooses $V_S \approx V_L$, and a high K_{eff} produces according to Eq. (4) very low equilibrium concentrations $[B]_{eq}$ and thus unacceptable long retention times. Usually the problem is handled with solvent mixtures that reduce the free binding enthalpy. In this paper we test polymer coatings that are able to shield the surface silanol groups against the interaction with proton accepting analytes. In principle, the coatings work, see Table 1. However, a large amount of polymer is necessary in order to obtain a significant effect, especially in the case of DVB-coating. TBB works much better and reduces the effective equilibrium constant into the range of K_{eff} = 1–100 which is acceptable for chromatographic separations. Especially the acidic surface centers are blocked by TBB so that the equilibrium constants of the bases AO and 1-DBA are strongly reduced against unshielded silica beads, whereas the acidic adsorptive LC is less affected. The success of TBB-coating in chromatography is exemplary shown in Fig. 4 for 1-DBA and 3-DBA. The two isomers are clearly separated in a HPLC-column with retention times 3-DBA < 1-DBA as expected from the equilibrium constants of adsorption.

4.2. Spectroscopic characterization of the adsorbed state

In order to assign the nature of the adsorbates BS we investigated the UV/vis-absorption and fluorescence spectra as well as the fluorescence anisotropies and decay curves. Table 2 summarizes some photophysical data of the adsorptives in solution. After addition of silica the systems became turbid, but this unwanted effect was minimized by high V_L/V_S – ratios and solvents that approach the refractive index of the silica beads. Despite these precautions the samples were still light scattering. However, the scattering anisotropies reached almost unity ($r_s \approx 0.95$) so that distortions of the absorption spectra or fluorescence anisotropies by multiple scattering were of minor importance.

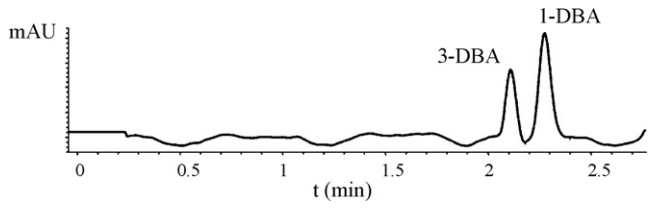

Fig. 4. Chromatogram of a 1:1 mixture of 1-DBA and 3-DBA in CH/isopropanol = 98.5/1.5 (V/V); using TBB-coated silica as stationary phase. Flow rate = 2 ml/min.

4.2.1. Acridine orange (AO)

The molecule with the highest basicity, was adsorbed on uncoated and coated silica beads as protonated species BH^+. Not a trace of the dimer $(BH^+)_2$ was found under our experimental conditions. Fig. 5 shows fluorescence excitation and emission spectra on uncoated silica. Comparison with the spectra in solution, see Fig. 6, gives evidence of adsorbed AOH^+, as well as of the absence of the first prominent absorption band of the neutral base AO at υ_{max} = 23,300 cm^{-1}. The F- and Exc-results on coated silica are assigned in the same way, see Fig. 7, with the slight restriction on DVB–silica, where small contributions of neutral AO were found. Also the mean fluorescence decay time of the adsorbate is the same as in acidic solution. Slight deviations from first order decay are observed, but these deviations are more or less the rule in adsorbates because of the slow individual environmental relaxation processes after excitation.

4.2.2. 1,2,7,8-Dibenzacridine (1-DBA)

The fluorescence emission and excitation spectra of 1-DBA adsorbed from CH on silica beads are given in Fig. 8. The spectra were recorded in a fluorescence cell in presence of CH (for details see Section 2). Some of the beads were fixed by electrostatic adhesion at the cell wall. By proper alignment of the spectrometer we could measure the bead spectra almost free of equilibrated 1-DBA remaining in solution. The results are presented in the bot-

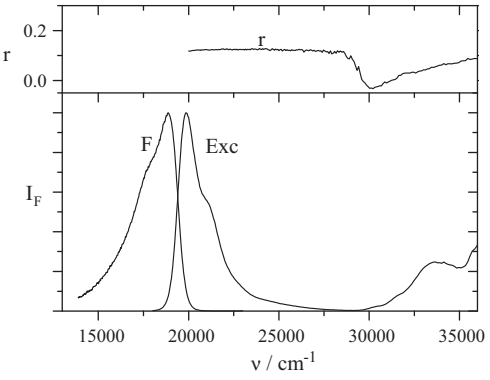

Fig. 5. Fluorescence emission (F), excitation (Exc), and anisotropy (r_F) spectra of AO adsorbed from dry DCM on uncoated silica beads, loading = 1.30×10^{-6} mol/g SiO_2. The fluorescence spectrum is excited at $\tilde{\upsilon}_{ex}$ = 23, 300 cm^{-1} and the excitation and anisotropy spectra are observed at $\tilde{\upsilon}_{em}$ = 17, 900 cm^{-1}.

Table 2
Fluorescence and first prominent absorption transition energies (M = maximum, S = shoulder, 0–0 = zero-to-zero transition), fluorescence decay times τ_F (under air), and steady-state fluorescence anisotropies r (in glycerol) of the investigated fluorophores in solution.

Fluorophore	Solvent	υ_F (cm^{-1})	υ_{abs} (cm^{-1})	τ_F (ns)	r_F
AO	Acidic ethanol (BH^+)	18,900 (M)	20,200 (M)	3.1	0.34
	Alkaline ethanol (B···H)	18,000 (M)	23,300 (M)	7.3	
1-DBA	Acidic ethanol (BH^+)	22,100 (F_1, M)	23,400 (A_1, 0–0)	6.7	0.34
	Ethanol (B···H)	25,000 (F_2, 0–0)	25,200 (A_2, 0–0)	8.0	0.18[a]
	Cyclohexane (B)	25,300 (F_3, 0–0)	25,500 (A_3, 0–0)	7.4	–
3-DBA	Acidic ethanol (BH^+)	20,000 (M)	23,400 (0–0)	11.8	0.19
	Ethanol (B)	25,300 (0–0)	25,300 (0–0)	9.7	
	Cyclohexane (B)	25,300 (0–0)	25,300 (0–0)	7.9	
LC	Alkaline ethanol (A^-)	18,200 (M)	22,500 (S)	–	–
	Acidic ethanol (AH_2^+)	19,000 (S)	25,000 (S + M)		
		21,000 (M)			
	Ethanol (AH···O)	21,700 (M)[b]	26,000 (M)	1.04[b]	0.29
	DCM (AH)	22,700 (M)[c]	26,200 (M)	0.61[c]	

Note: B and AH are the neutral species, B···H and AH···O are the hydrogen bonded species, BH^+ and A^- are the protonated or deprotonated species of the probes.
[a] In rigid solvent at $T = 77$ K [34].
[b] From Ref. [39].
[c] From Ref. [40].

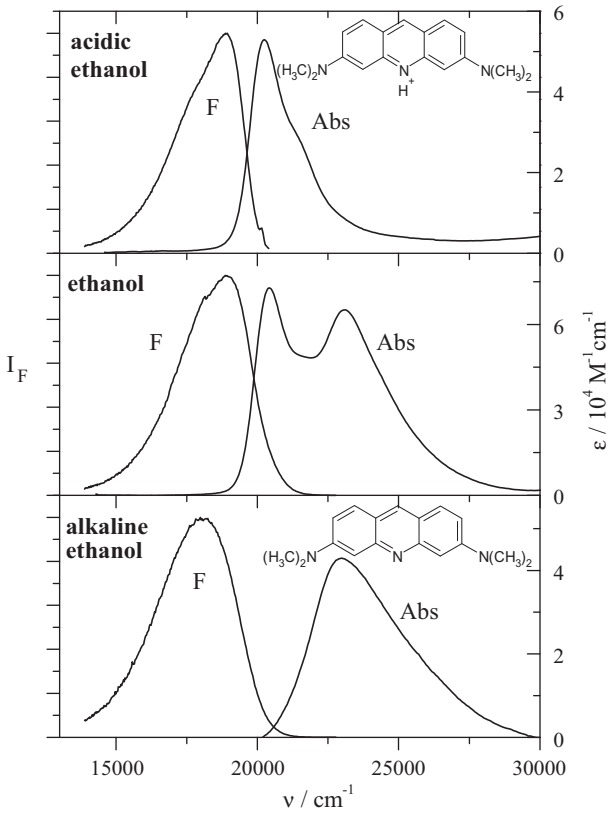

Fig. 6. Absorption (Abs) and fluorescence (F) spectra of AO in ethanol ($C = 3.90 \times 10^{-6}$ M) at different pH-values. Acidic ethanol (the fluorescence spectrum is excited at $\tilde{\upsilon}_{ex} = 20,200\,cm^{-1}$), neutral ethanol ($\tilde{\upsilon}_{ex} = 23,000\,cm^{-1}$) and alkaline ethanol ($\tilde{\upsilon}_{ex} = 23{,}000\,cm^{-1}$).

tom part of Fig. 8. Two different species 1 and 2 contribute to the fluorescence spectrum and by comparing the band positions with those in ethanol at different pH values (see Table 2) it can be concluded that the broad band of species 1 (labelled as F_1) at $\tilde{\nu}_{F,max} = 22,300\,cm^{-1}$ is due to the protonated form of 1-DBA (BH^+) adsorbed at the bead, and the emission band of species 2 (labelled as F_2) at $\tilde{\nu}_{F,0-0} = 24,950\,cm^{-1}$ is due to the H-bonded adsorbed species B···H. The intensity of F_1 dominates over F_2. The excitation spectrum Ex_1 for the F_1-fuorescence (detected at $\upsilon_{ex} = 20{,}000\,cm^{-1}$, i.e. outside the fluorescence of B···H) shows the first absorption band of BH^+ (labelled as A_1) but even more intense

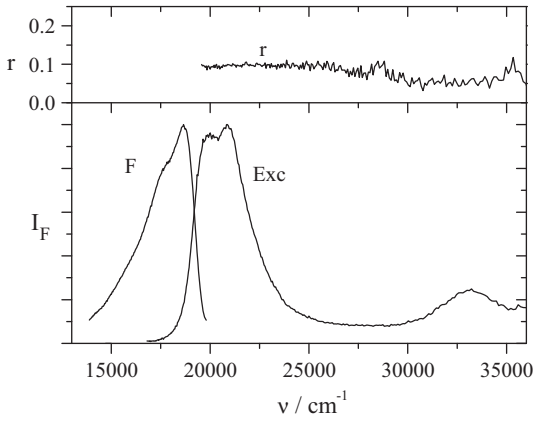

Fig. 7. Fluorescence emission (F), excitation (Exc), and anisotropy (r_F) spectra of AO adsorbed from dry DCM on DVB-coated silica beads, loading = 1.30×10^{-6} mol/g SiO_2. The fluorescence spectrum is excited at $\tilde{\upsilon}_{ex} = 20{,}000\,cm^{-1}$ and the excitation and anisotropy spectra are observed at $\tilde{\upsilon}_{em} = 14{,}300\,cm^{-1}$.

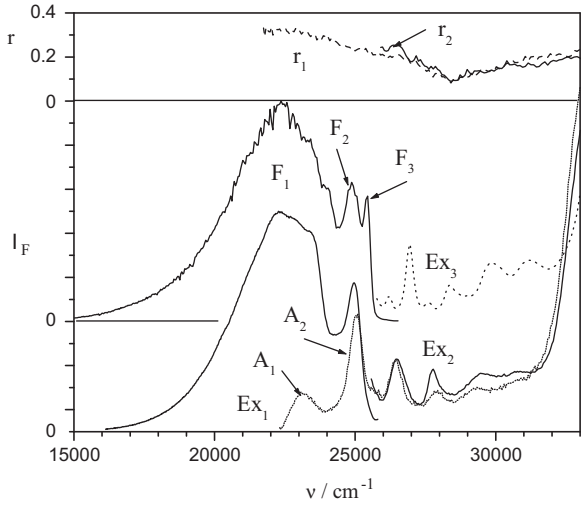

Fig. 8. Fluorescence (F), excitation (Exc), and anisotropy (r_F) spectra of 1-DBA adsorbed from dry CH on unpretreated silica beads, loading = 4.4×10^{-6} mol/g SiO_2. Bottom: Particles at the cell wall. Fluorescence spectrum is excited at $\tilde{\upsilon}_{ex} = 26{,}500\,cm^{-1}$. Excitation spectrum Exc_1 is observed at $\tilde{\upsilon}_{em} = 19{,}200\,cm^{-1}$, Exc_2 at $\tilde{\upsilon}_{em} = 24,900\,cm^{-1}$. Middle: Particles in suspension. Fluorescence spectrum is excited at $\tilde{\upsilon}_{ex} = 26{,}880\,cm^{-1}$. Exc_1 is observed at $\tilde{\upsilon}_{em} = 20{,}000\,cm^{-1}$, Exc_2 at $\tilde{\upsilon}_{em} = 24{,}900\,cm^{-1}$. Top: Anisotropy excitation r_1 is observed at $\tilde{\upsilon}_{em} = 20,000\,cm^{-1}$, r_2 at $\tilde{\upsilon}_{em} = 24{,}900\,cm^{-1}$.

Table 3
Fluorescence decay times τ_F, steady-state fluorescence anisotropies (r_F), and the amplitudes A of 1-DBA and AO (uncoated silica + cyclohexane) under air, $\upsilon_{ex} = 27{,}000\,cm^{-1}$.

Probe	υ_{em} (cm^{-1})	τ_F (ns)	Amplitude	(r_F)
1-DBA	24,900	4.3	0.07	0.18
		8.3	0.93	
	20,800	2.4	−0.22	0.31
		7.2	0.60	
		9.5	0.18	
AO	17,900	2.7	0.82	0.12
		4.4	0.18	
LC	21,100	–	–	0.29

also the first absorption band of B···H (labelled as A_2). So the A_1/A_2 ratio is opposite to the F_1/F_2 ratio. The higher energetic vibronic sub-bands of Ex_1 are identical with the excitation spectrum Ex_2 that was measured at F_2 (because of primary light scattering, the Ex_2-spectrum could not be measured in the A_2-region). These results prove the presence of two adsorbed ground state species, B···H and BH^+, and support the following excited state acid–base reaction

$$B\cdots H\text{–}OSi + h\upsilon \rightarrow [B\cdots H]^*\text{–}OSi \rightarrow [BH^+]^*\text{–}OSi \quad (7)$$

known from reactions in liquids when the acidity of excited BH^+ is much lower than in the ground state. This is the case for acridine and its derivatives, see Table 1. However, reaction (7) occurs only for part of adsorbed B···H, since we find for the (remaining) B···H adsorbates the very similar fluorescence lifetime $\tau_F = 8.3$ ns as in ethanolic solution with $\tau_F = 8.0$ ns (values in air, compare Tables 2 and 3). Thus, that part of B···H that undergoes reaction (7) must disappear faster than the resolution of our setup whereas the remaining part does not react at all. On the other hand we find a rising component in the fluorescence of adsorbed BH^+ that has no equivalent counterpart in the decay of adsorbed B···H. We cannot give a final explanation for this result but it should be mentioned that environmental relaxation processes after excitation occur on surfaces in the ns-range [41,42].

The middle of Fig. 8 presents the spectra of beads inside the well-stirred suspension of CH. The spectra are noisy because of the fluctuating bead number in the excited sample volume. In addition to the bottom spectra one finds a third fluorescent species 3 with the highest energetic maximum at $\upsilon_{F,0-0} = 25{,}400\,cm^{-1}$ (labelled as F_3). The associated excitation spectrum Ex_3 originates at $\upsilon_{ex} = 25{,}500\,cm^{-1}$ (=A_3) and is shifted against Ex_2 by $300\,cm^{-1}$ to the blue. The band system 3 is assigned to the adsorptive B remaining dissolved in the adsorption equilibrium.

From Table 1 we know that the adsorption equilibrium of 1-DBA is shifted to the dissolved state in presence of small amounts of water. Fig. 9 shows that also the nature of the adsorbates changes upon adsorption from not dried CH. The fluorescence is now dominated by adsorbed B···H and dissolved B, whereas almost no BH^+ is formed. Thus reaction (7) occurs only with unshielded silanol groups.

4.2.3. 3,4,5,6-Dibenzacridine (3-DBA)

3,4,5,6-Dibenzacridine (3-DBA) interacts only little with the silica beads because of the sterically shielded nitrogen center. The equilibrium constant of adsorption is low and comparable to condensed aromatic hydrocarbons without functional groups such as anthracene, pyrene or perylene, where $K_{eff} = 1$–10 on silica, and $K_{eff} = 20$–100 on hydroxyl-covered alumina. [23,26]. Contrary to 1-DBA, no spectral signature of an H-bound adsorbate B···H could be detected for 3-DBA on silica. This is in accordance with the fluorescence in ethanolic solution that also shows no H-induced red-shift against aprotic solvents, see Table 2.

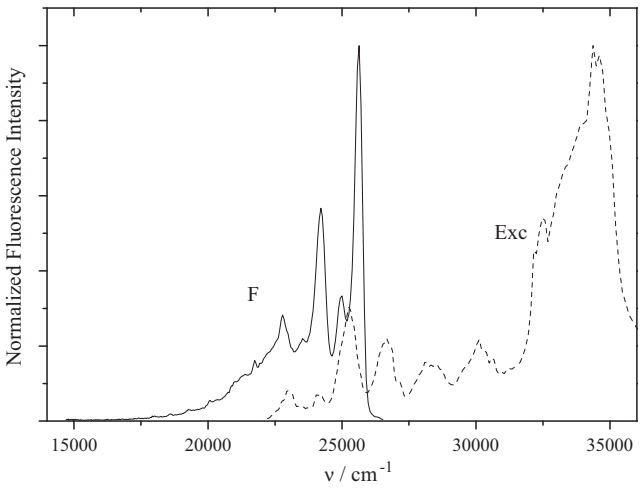

Fig. 9. Fluorescence (*F*) and excitation (Exc) spectra of 1-DBA adsorbed from not dry CH on unpretreated silica beads, loading = 4.4×10^{-6} mol/g SiO_2. The fluorescence spectrum is excited at $\tilde{\upsilon}_{ex} = 26{,}880\,cm^{-1}$, the excitation spectrum (Exc) is observed at $\tilde{\upsilon}_{em} = 2{,}1300\,cm^{-1}$.

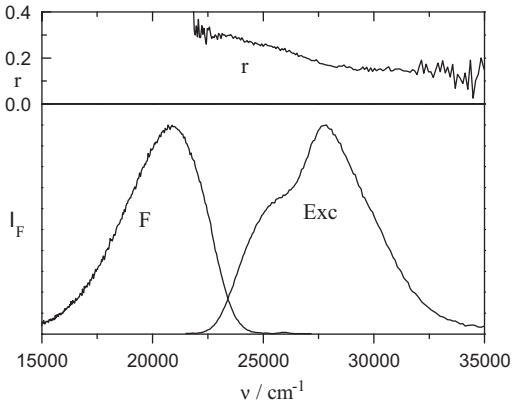

Fig. 10. fluorescence (*F*), excitation (Exc) and anisotropy (r_F) spectra of LC adsorbed from DCM on unpretreated silica beads, loading = 3.4×10^{-6} mol/g SiO_2. The fluorescence spectrum is excited at $\tilde{\upsilon}_{ex} = 29{,}000\,cm^{-1}$, the excitation and the anisotropy spectra are observed at $\tilde{\upsilon}_{em} = 21{,}100\,cm^{-1}$.

4.2.4. Lumichrome (LC)

Lumichrome (LC) is a multifunctional molecule with proton-donor sites at N(1)H and N(3)H, and proton-acceptor sites at N(10) and at the carbonyl groups C(2)O and C(4)O, (see Fig. 2). It is reasonable to expect that adsorbed LC is able to form different hydrogen bonds or proton transfer states with the surface silanol groups of silica. According to theoretical calculations, the charge densities on the N(1) and N(3) nitrogen atoms are almost identical in the ground state resulting in very similar values of the de-protonation constants pK_a [43,44]. The experimental value for N(1)H is $pK_a = 8.6$ [45], so that LC is a very weak acid in its electronic ground state. The acidity at N(1) increases strongly in the first excited singlet state resulting in $pK_a^* = 3.6$. Despite a variety of potential surface reactions, the spectra of adsorbed LC look very simple, see Fig. 10. The broad fluorescence emission band with $\upsilon_{F,max} = 21{,}000\,cm^{-1}$ is slightly red-shifted against its position in ethanol, see Table 2, or on cellulose, where $\nu_{max} = 21{,}700\,cm^{-1}$ is reported [35]. In both environments the fluorescence was assigned to H-bonded LC. It is reasonable to adopt this assignment for LC adsorbed on silica. However, we also discuss LCH^+, protonated at N(10), as second fluorescent adsorbate in order to account for the low energetic broad fluorescence, and especially for the positions of the absorption bands at $\nu_{sh} \approx 25{,}000\,cm^{-1}$ (shoulder) and $\nu_{max} = 28{,}000\,cm^{-1}$

which are very comparable to the positions in acidic ethanol. In solution, the high N(1)-acidity and high N(10)-basicity of excited LC* causes double-proton transfer with rearrangement of the entire electronic structure to yield the flavin tautomer of LC (see Fig. 2) as in the case of acetic acid addition to LC in ethanol [46]. A comparable reaction can take place also on silica with its effective acidity constant of $pK_a = 5–6$ [47].

4.3. Fluorescence polarization

The fluorescence spectra of the adsorbates are highly polarized and reach for protonated 1-DBA and LC the limiting anisotropies $r_F = 0.32$ and 0.29, respectively, of solutions in highly viscous glycerol (see Figs. 8, 10, and Tables 2 and 3). H-bound 1-DBA reaches a lower value of $r_F = 0.19$ which is also the limit in highly viscous glass [34], because L_a and L_b with orthogonal orientations of their transition dipoles are excited simultaneously. According to these results the adsorbates are rotationally immobile during their fluorescence lifetimes. However, it cannot be concluded from these data that the adsorbates are immobile at all. For acridines one finds translational diffusion taking place in the microsecond time domain on silica gels covered with silanol groups [42], and the diffusion controlled adsorption–desorption reactions take place in the time range of seconds.

The anisotropy of adsorbed AO raises some unanswered questions. We find $r_F = 0.12$ on uncoated silica, $r_F = 0.09$ on DVB–silica (200 mg), and $r_F = 0.02$ on TBB–silica. Since the experimental r_F are mean values of adsorbed and dissolved ($r_F \approx 0$) AO, the influence of coating can be ascribed to the smaller K_{eff}-values (the contribution of dissolved AO can be seen in Fig. 7 as second excitation maximum). However, the maximum r_F on uncoated silica is far away from $r_F = 0.34$ in glycerol, where the molecule is dissolved in its protonated state. It cannot be excluded, but it is unlikely that the excited adsorbate undergoes significant rotational diffusion during its short lifetime of 3 ns. Under our experimental conditions the molecule is quantitatively adsorbed with the highest binding energy of all adsorbates. Since also the Stokes shift between absorption and fluorescence maximum is reduced from 1300 cm^{-1} in acidified ethanol to 900 cm^{-1} on silica it is reasonable to assume that the adsorbate is strongly fixed. Starting from the reduced Stokes shift we take into account the possibility of homo resonance energy transfer (ET) as source of fluorescence depolarization. The fluorescent electronic state of AOH^+ is fully allowed with a maximum decadic extinction coefficient of $\varepsilon = 53{,}000\ cm^2\ mmol^{-1}$. From the spectra of Fig. 5 we obtain the Förster overlap integral $J = 3.5 \times 10^{-14}\ cm^6\ mmol^{-1}$ and finally the Förster radius $R_0 = 4.0$ nm. This quantity is compared with the average distance between the adsorbed AOH^+ ions, $\langle\rho\rangle = 8.2$ nm, estimated as upper limit with the assumption that the adsorbate is equally distributed over the volume of the highly porous silica. A more realistic estimate assumes that the ions are strongly fixed in the outer regions of the beads. Then the mean distance becomes smaller and ET will now be the most important source of fluorescence depolarization.

In principle, also the other adsorbates are subject to ET. However, their overlap integrals are much smaller than that of AOH^+, and additionally part of 1-DBA escapes from ET by reaction (7).

5. Conclusion

According to our spectroscopic investigations the interaction of dissolved poly-condensed aza-aromatic molecules with porous silica beads utilized as stationary chromatographic phases is mainly controlled by the basicity at the nitrogen centers of the aromatics. Increasing basicity increases the effective equilibrium constant K_{eff} of adsorption. The polarizability of the aromatic π-electron system is of secondary importance, as shown by comparing molecules with equal π-skeletons but different accessibilities of their basic center.

The activity of the beads is controlled by the accessibility of the silanol groups at the solid/liquid interface. Free silanol groups are stronger proton donors than groups that are screened from the aromatics by adsorbed water.

Substantial shielding of the silanol groups is achieved with polymer coatings. This procedure reduces the equilibrium constants of adsorption by two to three orders of magnitude and makes the stationary phases suitable for HPLC.

Acknowledgements

We thank Prof. Dr. K. Albert, Dr. U. Skogsberg and Dr. G. Fischer (Institute of Organic Chemistry, Tübingen University) for supplying the DVB-coated silica and HPLC measurements.

References

[1] D.V. McCalley, LC–GC Eur. 12 (1999) 638.
[2] Li Zengbiao, S.C. Rutan, Solvatochromic studies of the surface polarity of silica under normal-phase conditions, Anal. Chim. Acta 312 (1995) 127–139.
[3] B. Pfleiderer, E. Bayer, Silanediol groups of the silica gel nucleosil: active sites involved in the chromatographic behaviour of bases, J. Chromatogr. A 468 (1989) 67–71.
[4] K.G. Wahlund, A. Sokolowski, Reversed-phase ion-pair chromatography of antidepressive and neuroleptic amines and related quaternary ammonium compounds, J. Chromatogr. 151 (1978) 299–310.
[5] B.A. Person, B.L. Karger, in: H. Engelhardt (Ed.), Practice of High Performance. Liquid Chromatography, Springer, Heidelberg, 1986, p. 201.
[6] S.M. Hansen, P. Helboe, M. Thomson, Bare silica, dynamically modified with long-chain quaternary ammonium ions – the technique of choice for more reproducible selectivity in reversed-phase high-performance liquid chromatography, J. Chromatogr. A 544 (1991) 53–76.
[7] J. Nawrocki, B. Buszewski, Influence of silica surface chemistry and structure on the properties, structure and coverage of alkyl-bonded phases for high-performance liquid chromatography, J. Chromatogr. A 449 (1988) 1–24.
[8] L.C. Tan, P.W. Carr, Study of retention in reversed-phase liquid chromatography using linear solvation energy relationships: II. The mobile phase, J. Chromatogr. A 799 (1998) 1–19.
[9] M.L. Hetem, Van de Ven, J. de Haan, C. Cramers, K. Albert, E. Bayer, Study of the changes in mono-, di- and trifunctional octadecyl-modified packings for reversed-phase high-performance liquid chromatography with different eluent compositions, J. Chromatogr. A 479 (1989) 269–295.
[10] L. Sander, S.A. Wise, Synthesis and characterization of polymeric C18 stationary phases for liquid chromatography, Anal. Chem. 56 (1984) 504–510.
[11] H. Engelhardt, A.M. Cunat-Walter, Preparation and stability tests for polyacrylamide-coated capillaries for capillary electrophoresis, J. Chromatogr. A 716 (1995) 27–33.
[12] B. Yan, J.S. Zhao, J. Brown, F. Blackwell, W.P. Carr, High-temperature ultrafast liquid chromatography, Anal. Chem. 72 (2000) 1253–1262.
[13] J. Zhao, W.P. Carr, Synthesis and evaluation of an aromatic polymer-coated zirconia for reversed-phase liquid chromatography, Anal. Chem. 71 (1999) 5217–5224.
[14] E. Boschetti, Advanced sorbents for preparative protein separation purposes, J. Chromatogr. A 658 (1994) 207–236.
[15] D. Bentrop, J. Kohr, J. Engelhardt, Poly(methylglutamate)-coated surfaces in HPLC and CE, Chromatographia 32 (1991) 171–178.
[16] S. Durie, K. Jerabek, C. Mason, C.D. Sherrington, One-pot synthesis of branched poly(styrene-divinylbenzene) suspension polymerized resins, Macromolecules 35 (2002) 9665–9672.
[17] K. Jerabek, Characterization of swollen polymer gels using size exclusion chromatography, Anal. Chem. 57 (1985) 1598–1602.
[18] C.G. Huber, G. Kleindienst, G.K. Bonn, Application of micropellicular polystyrene/divinylbenzene stationary phases for high-performance reversed-phase liquid chromatography electrospray-mass spectrometry of proteins and peptides, Chromatographia 44 (1997) 438–448.
[19] R.V. Law, D.C. Sherrington, C.E. Snape, Quantitative solid state ^{13}C NMR studies of highly cross-linked poly(divinylbenzene) resins, Macromolecules 30 (1997) 2675–2868.
[20] R. Partch, S. Brown, Aerosol and solution modification of particle–polymer interfaces, J. Adhesion 67 (1998) 259–276.
[21] S.G. Allenmark, S. Andersson, P. Möller, D. Sanchez, A new class of network-polymeric chiral stationary phases, Chairality 7 (1995) 248–256.
[22] S. Andersson, S. Allenmark, P. Möller, B. Persson, D. Sanchez, Chromatographic separation of enantiomers on N,N′-diallyl-L-tartardiamide-based network – polymeric chiral stationary phases, J. Chromatogr. A 741 (1996) 23–31.

[23] D. Oelkrug, M. Radjaipour, H. Erbse, Lumineszenz adsorbierter Aromaten I. Zur. assoziation von physikalisch adsoebiertem Pyren und Naphthalin auf. Metalloxidoberflächen, Z. Phys. Chem. N.F 88 (1974) 23–36.
[24] R.K. Bauer, P. de Mayo, W.R. Ware, K.C. Wu, Surface photochemistry. The photophysics of pyrene adsorbed on silica gel, alumina, and calcium fluoride, J. Phys. Chem. 86 (1982) 3781–3789.
[25] K.A. Zachariasse, in: M. Anpo, T. Matsuura (Eds.), Photochemistry on Solid Surfaces, Studies in Surface Science and Catalysis, Elsevier, Amsterdam, 1989, p. 48.
[26] D. Oelkrug, H. Erbse, M. Plauschinat, Z. Phys. Chem. N.F 96 (1975) 283;
D. Oelkrug, M. Radjaipour, Z. Phys. Chem. N.F 123 (1980) 163.
[27] D. Oelkrug, G. Schrem, I. Andrä, Z. Phys. Chem. N.F 106 (1977) 197;
K. Rempfer, S. Uhl, D. Oelkrug, Luminescence studies of acid–base interactions on metal oxide catalysts, J. Mol. Struct. 114 (1984) 225–228.
[28] J.B.F. Lloyed, Nitrogen heterocycle and polynuclear hydrocarbon fluorescence and. adsorption effects in the presence of silica gel. Applications in high-pressure liquid and microcolumn chromatography, Analyst 100 (1975) 529–539.
[29] P. Hite, R. Krasnansky, J.K. Thomas, Spectroscopic investigations of surfaces by using aminopyrene, J. Phys. Chem. 90 (1986) 5795–5799.
[30] S.A. Samchuk, N.P. Smirnova, A.M. Eremenko, Spectral parameters and. photoprotolytic interactions for acridine adsorbed on silica, J. Appl. Spectrosc. 52 (1990) 195–198;
N.P. Smirnova, A.M. Eremenko, A.A. Chuiko, Fluorescence spectra of adsorbed heteroaromatic molecules at selective laser excitation, J. Mol. Struct. 266 (1992) 417–422.
[31] S. Suzuki, T. Fujii, in: M. Anpo, T. Matsuura (Eds.), Photochemistry on Solid Surfaces, Elsevier, Amsterdam, 1989, p. 79.
[32] D. Oelkrug, W. Flemming, R. Füllemann, R. Günther, W. Honnen, G. Krabichler, M. Schäfer, S. Uhl, Pure Appl. Chem. 58 (1986) 1207–1218.
[33] G. Fischer, U. Skogsberg, S. Bachmann, H. Yuksel, S. Steinbrecher, E. Plies, K. Albert, Synthesis, characterization, and evaluation of divinylbenzene-coated spherical, nonporous silica, Chem. Mater. 15 (2003) 4394–4400.
[34] H.-H. Perkampus, A. Knop, J.V. Knop, Spectrochim. Acta A 25 (1969) 1589–1602.
[35] M. Sikorski, E. Sikorska, I.V. Khmelinskii, R.G. Moreno, J.L. Bourdelande, A. Siemiarczuk, Photophysics of lumichrome on cellulose, J. Photochem. Photobiol. A 156 (2003) 267–271.
[36] A. Weller, Z. Elektrochem, Ber. Bunsenges. Phys. Chem. 61 (1957) 956.
[37] A. Gafni, L. Brand, Chem. Phys. Lett. 58 (1978) 346–350.
[38] V. Zanker, Phys. Chem. 199 (1952) 225.
[39] M. Sikorski, D. Purkata, M.I. Rak, I. Khmelinskii, D.R. Worrall, S.L. Williams, J. Hernando, J.L. Bourdelande, J. Koput, E. Sikorska, Spectroscopy and photophysics of dimethyl-substituted alloxazines, J. Photochem. Photobiol. A 200 (2008) 148–160.
[40] E. Sikorska, H. Szymusiak, I.V. Khmelinskii, A. Koziolowo, J.S. Larsen, M. Sikorski, Spectroscopy and photophysics of alloxazines studied in their ground and first excited singlet states, J. Photochem. Photobiol. A 158 (2003) 45–53.
[41] S. Uhl, K. Rempfer, H.-J. Egelhaaf, B. Lehr, D. Oelkrug, Fluorescence characterization of acid–base interaction and mobility at chromatographic interfaces, Anal. Chim. Acta 303 (1995) 17–23.
[42] H.-J. Egelhaaf, D. Oelkrug, A. Ellwanger, K. Albert, Investigation of structure and mobility of silica bonded stationary acridine phase by means of fluorescence and NMR spectroscopy, J. High Resolut. Chromatogr. 21 (1998) 11–17.
[43] A. Koziolowa, Photochem. Photobiol. 29 (1979) 459–471.
[44] M. Sikorski, E. Sikorska, A. Koziolowa, R.G. Moreno, J.L. Bourdelande, R.P. Steer, F. Wilkinson, J. Photochem. Photobiol. B 60 (2001) 114–119.
[45] M. Sikorski, E. Sikorska, I.V. Khmelinskii, R.G. Moreno, J.L. Bourdelande, A. Siemiarczuk, J. Photochem. Photobiol. A 156 (2003) 267–271.
[46] M. Sun, T.A. more, P.-S. Song, Molecular luminescence studies of flavines. I. Excited states of flavines, J. Am. Chem. Soc. 94 (1972) 1730–1740.
[47] H.A. Benesi, J. Am. Chem. Soc. 78 (1956) 5490–5494.